


Bioengineered gold nanoparticles targeted to mesenchymal cells from patients with bronchiolitis obliterans syndrome does not rise the inflammatory response and can be safely inhaled by rodents

Emanuela Cova, Simona Inghilleri, Laura Pandolfi, Monica Morosini, Sara Magni, Miriam Colombo, Davide Piloni, Chiara Finetti, Gabriele Ceccarelli, Laura Benedetti, Maria Gabriella Cusella, Manuela Agozzino, Fabio Corsi, Raffaele Allevi, Simona Mrakic-Sposta, Sarah Moretti, Simona De Gregori, Davide Prospero & Federica Meloni


To cite this article: Emanuela Cova, Simona Inghilleri, Laura Pandolfi, Monica Morosini, Sara Magni, Miriam Colombo, Davide Piloni, Chiara Finetti, Gabriele Ceccarelli, Laura Benedetti, Maria Gabriella Cusella, Manuela Agozzino, Fabio Corsi, Raffaele Allevi, Simona Mrakic-Sposta, Sarah Moretti, Simona De Gregori, Davide Prospero & Federica Meloni (2017): Bioengineered gold nanoparticles targeted to mesenchymal cells from patients with bronchiolitis obliterans syndrome does not rise the inflammatory response and can be safely inhaled by rodents, *Nanotoxicology*, DOI: [10.1080/17435390.2017.1317862](https://doi.org/10.1080/17435390.2017.1317862)

To link to this article: <http://dx.doi.org/10.1080/17435390.2017.1317862>

 View supplementary material 

 Accepted author version posted online: 18 Apr 2017.
Published online: 27 Apr 2017.

 Submit your article to this journal 

 Article views: 24

 View related articles 

 View Crossmark data 

Bioengineered gold nanoparticles targeted to mesenchymal cells from patients with bronchiolitis obliterans syndrome does not rise the inflammatory response and can be safely inhaled by rodents

Emanuela Cova^{a*}, Simona Inghilleri^{a*}, Laura Pandolfi^b, Monica Morosini^a, Sara Magni^a, Miriam Colombo^b, Davide Piloni^c, Chiara Finetti^b, Gabriele Ceccarelli^d, Laura Benedetti^d, Maria Gabriella Cusella^d, Manuela Agozzino^e, Fabio Corsi^{f,g}, Raffaele Allevi^f, Simona Mrakic-Spota^h, Sarah Moretti^h, Simona De Gregoriⁱ, Davide Prosperi^b and Federica Meloni^c

^aClinica di Malattie dell'Apparato Respiratorio, IRCCS Fondazione Policlinico San Matteo, Pavia, Italy; ^bDipartimento di Biotecnologie e Bioscienze, Università di Milano-Bicocca, Milano, Italy; ^cDipartimento di Medicina Interna, Unità di Pneumologia, Università degli Studi di Pavia, Pavia, Italy; ^dIstituto di Anatomia Umana, Dipartimento di Salute Pubblica, Medicina Sperimentale e Forense, Università degli Studi di Pavia, Pavia, Italy; ^eCentro per le Malattie Cardiovascolari Ereditarie, IRCCS Fondazione Policlinico San Matteo, Pavia, Italy; ^fDipartimento di Scienze Biomediche e Cliniche L. Sacco, Università degli Studi di Milano, Pavia, Italy; ^gChirurgia Senologica, ICS Maugeri S.p.A. SB, Pavia, Italy; ^hIstituto di Bioimmagini e Fisiologia Molecolare, Consiglio Nazionale delle Ricerche (CNR), Segrate, Milano, Italia; ⁱS.S.di Farmacocinetica Clinica e Sperimentale, IRCCS Fondazione Policlinico San Matteo, Pavia, Italy

ABSTRACT

The use of gold nanoparticles (GNPs) as drug delivery system represents a promising issue for diseases without effective pharmacological treatment due to insufficient local drug accumulation and excessive systemic toxicity. Bronchiolitis obliterans syndrome (BOS) represents about 70% of cases of chronic lung allograft dysfunction, the main challenge to long-term lung transplantation. It is believed that due to repeated insults to epithelial bronchiolar cells local inflammatory response creates a milieu that favors epithelial-mesenchymal transition and activation of local mesenchymal cells (MCs) leading to airway fibro-obliteration. In a previous work, we engineered GNPs loaded with the mammalian target of rapamycin inhibitor everolimus, specifically decorated with an antibody against CD44, a surface receptor expressed by primary MCs isolated from bronchoalveolar lavage of BOS patients. We proved *in vitro* that these GNPs (GNP-HCe) were able to specifically inhibit primary MCs without affecting the bronchial epithelial cell. In the present work, we investigated the effect of these bioengineered nanoconstructs on inflammatory cells, given that a stimulating effect on macrophages, neutrophils or lymphocytes is strongly unwanted in graft airways since it would foster fibrogenesis. In addition, we administered GNP-HCe by the inhalatory route to normal mice for a preliminary assessment of their pulmonary and peripheral (liver, spleen and kidney) uptake. By these experiments, an evaluation of tissue toxicity was also performed. The present study proves that our bioengineered nanotools do not rise an inflammatory response and, under the tested inhalatory conditions that were used, are non-toxic.

ARTICLE HISTORY

Received 24 June 2016
Revised 23 February 2017
Accepted 3 April 2017

KEYWORDS





Targeted gold nanoparticles; bronchiolitis obliterans syndrome; inflammatory response; toxicity; inhalation

Introduction


Gold nanoparticles (GNPs) are among the most intensely studied nanomaterials due to their unique size-dependent electronic and optical properties (Biju et al., 2008; Mieszawska et al., 2013) combined with great potential in a broad range of biomedical applications (Giljohann et al., 2010; Liu & Ye, 2013). Indeed, GNPs exhibit multiple different properties of the gold core at the nanoscale, which make them applicable in medical imaging and therapy as contrast agents, targeted diagnostic tool, radio/photothermal therapeutics and as drug/gene delivery vehicles (Cole et al., 2015; Cooper et al., 2014; Heo et al., 2012; Zhao et al., 2014). Hydrophobic GNPs are produced by chemical reduction of gold salts to colloidal gold in the presence of a capping ligand in non-polar solvents, thus obtaining highly stable GNPs, usually ranging in size from 1 to 8 nm (Brust et al., 1994). However, further surface

functionalization is needed to provide them high biocompatibility and low cytotoxicity, which is normally obtained by amphiphile-polymer coating using polyethylene glycol (PEG) (Niidome et al., 2006). This functionalization prevents non-specific protein adsorption on GNPs *in vivo*, undesired uptake by the reticuloendothelial system and prolonged half-life (Niidome et al., 2006). In addition, when targeting to specific cell types is required, antibodies, peptides, aptamers and small molecule can be easily attached to their surface (El-Sayed et al., 2005; Heo et al., 2012).

We have recently developed a new nanovehicle aimed at inhalatory local treatment of bronchiolitis obliterans syndrome (BOS), which is the most frequent phenotype of chronic lung allograft dysfunction (CLAD), the major cause of poor outcomes after lung transplantation. The histological correlation of BOS is an obliterative bronchiolitis, characterized by a patchy submucosal fibrosis

CONTACT Emanuela Cova  e.cova@smatteo.pv.it  IRCCS Policlinico San Matteo Foundation, Viale Golgi, 19, 27100 Pavia, Italy; Davide Prosperi  davide.prosperi@unimib.it  NanoBioLab, Dipartimento di Biotecnologie e Bioscienze, Università di Milano-Bicocca, Milano, Italy

*These authors contributed equally to this work.

 Supplemental data for this article can be accessed [here](#).

causing total occlusion of tracts of the bronchiolar lumen (Weigt et al., 2013). Although the exact pathogenesis of BOS is still unknown, it is believed that an insult to the epithelium triggers an amplification of both innate and adaptive immune responses. Chronic inflammatory signals cause an unbalance of local response from graft tolerance to allo- or auto-immunity, mainly of the Th-17 pattern, driving a typical neutrophilic inflammation (Vanaudenaerde et al., 2011; Verleden et al., 2015). Activated neutrophils can further damage the epithelium releasing reactive oxygen species, chemokines, alarmins and metalloproteinases (Hardison et al., 2009; Khatwa et al., 2010). This chronic neutrophilic inflammation induces reparative fibrosis with the proliferation of mesenchymal cells (MCs) (Badri et al., 2011; Ramirez et al., 2008; Todd & Palmer, 2011).

In a previous work (Cova et al., 2015), we designed a new nano-vehicle-based treatment to specifically target MCs intended to be administered by inhalation. GNPs were loaded with everolimus, a synthetic drug which inhibits the mammalian target of rapamycin (mTOR), a kinase that regulates cell growth and metabolism in MCs. To specifically address GNPs to MC cells in lung tissue, we decided to functionalize the GNP surface with a monoclonal antibody (mAb) against CD44. Indeed, this glycoprotein is highly expressed on the surface of MC cells isolated from bronchoalveolar lavage (BAL) and by cells of fibroblast foci that characterize the lung tissue of BOS patients (Cova et al., 2015). We demonstrated that GNPs targeted to MCs, not only significantly inhibited their proliferation *in vitro*, but also the effect was higher and longer lasting compared to treatment with the drug alone. In addition, GNPs did not affect alveolar epithelial cell viability thus opening an opportunity for local treatment in BOS (Cova et al., 2015). However, considering that BOS is the final result of a chronic pro-inflammatory insult, in view of a possible clinical translation, a crucial implication is to rule out if our nanoconstructs could enhance the activity of immune effectors, increasing the inflammatory response and oxidative stress in BOS patients. For this reason, in the present work, we aimed to determine the effect of our engineered drug-loaded nanoparticles on macrophages, neutrophils and lymphocytes with multiparameter *in vitro* assays by evaluating cytokine secretion, reactive oxygen species (ROS) production, cell viability and apoptosis. In order to simulate an inflamed microenvironment, we assayed the effect of our nanoconstructs also after appropriate stimulation of inflammatory cells. In addition, although several authors documented that (Geiser et al., 2013; Han et al., 2015; Sadauskas et al., 2009) the toxic effect of inhaled GNPs with size range similar to ours was limited, we studied the potential impact of repeated nanoparticles delivery by aerosolization on normal mice, evaluating the localization and toxicity on lungs and peripheral organs. The main experiments to assess the nanoparticles impact on inflammatory response have been performed in cell cultures with the aim to reduce animal utilization.

Materials and methods

Nanoparticle preparation

Water-soluble GNPs functionalized with anti-human CD44 and loaded with everolimus (GNP-HCe) were prepared according to our previously published protocol (Cova et al., 2015). Briefly, 6 nm diameter surfactant-coated GNPs were synthesized following the Brust protocol (Brust et al., 1994) and transferred in water solution undergoing a coating procedure with the amphiphilic polymer PMA obtained by reaction of 75% reacting groups of poly(isobutylene-*alt*-maleic anhydride) with dodecylamine (GNP@PMA) (Pellegrino et al., 2004). GNP@PMA (500 μ l of a 4 μ m solution),

Table 1. Nanoparticles used in *in vitro* and *in vivo* experiments.

	PMA polymer	PEG	AntiCD44 HC-mAb	Everolimus
GNP@PMA	X	–	–	–
GNP-HC	X	X	X	–
GNP-PEG	X	X	–	–
GNP-PEGe	X	X	–	X
GNP-HCe	X	X	X	X

were reacted with 2,2-(ethylenedioxy)bis(ethylamine) (EDBE, 80 μ l 0.05 M in deionized water) in the presence of 1-ethyl-3-(3-dimethylaminopropyl) carbodiimide (EDC, 20 μ l, 1 M in deionized water) for 2 h. The resulting nanoparticles were shaken for 4 h with 5 mg of *N*-succinimidyl-3-[2-pyridylthio]-propionate (SPDP). Next, the half chain of anti-human CD44 mAb (0.4 mg) and MeO-PEG500-SH were added and incubated at room temperature for 1 h, resulting in the antibody-functionalized nanoparticles (GNP-HC). Everolimus dissolved in ethanol (0.65 mg) was added to 1 mg of the washed and recollected GNP-HC solution and incubated overnight at 4 °C obtaining everolimus-loaded nanoparticles (GNP-HCe) with *ca.* 1 drug molecule per nanoparticle. PEG functionalized GNP were synthesized by reacting GNP@PMA (250 μ l of 4 μ m solution) with *O*-(2-Aminoethyl)-*O'*-methyl-PEG (PEG2000-NH₂, MW 2000, 27 μ l in 0.1 M water) in the presence of 1 M EDC (9.5 μ l), as previously reported (Cova et al., 2015). Dye-labeled nanoparticles were obtained using 0.5 M PMA labeled with AlexaFluor488 (AF488) for cell treatment or with IR820 dye for mice inhalation. Dyes were covalently linked to the polymer by amide bond formation between the amino group of the EDBE linker attached to the PMA polymer and the activated carboxyl group of the dye molecule. The chemical features of the nanoparticles synthesized in this work are summarized in Table 1.

Cell isolation and treatment

Macrophages were isolated from BAL of patients with hemoptysis *sine causa* by adhesion procedure. Briefly, 5×10^6 cells/well were seeded in 24-well plates in RPMI medium for 2 h at 37 °C to allow adhesion. For neutrophil isolation, a buffy coat sample from peripheral blood of donors was separated by gradient stratification with lympholyte (Cedarlane Laboratories, Burlington, ON, Canada). CD3+T cells were purified from peripheral blood of donors by negative magnetic beads separation (CD3+T-cell Isolation Kit, Miltenyi Biotec, Gergisch Gladbach, Germany). Macrophages were treated for 2 h with 25 μ g/ml of GNP-HCe or GNP-HC and with GNP-PEGe or GNP-PEG. The effect of nanoparticles was assayed after 48 h incubation by evaluating viability, IL-8 release and ROS production in both unstimulated and macrophages stimulated by adding 0.01 mg/ml lipopolysaccharide (LPS, Sigma-Aldrich, Milan, Italy). Long-time effect on macrophages viability and activity was also assessed at 7 and 10 d after nanoparticle treatment. Neutrophils were treated for 4 h with GNP-HC, GNP-HCe, GNP-PEG and GNP-PEGe. Activation was assayed by evaluating the elastase release, ROS production and apoptosis. Un-functionalized nanoparticles with or without drug inside, GNP-PEGe and GNP-PEG, respectively, were also tested on macrophages and neutrophils to assay possible stimulating action of the nanoparticles *per se*. CD3+T lymphocytes were treated with 25 μ g/ml of GNP-HC and GNP-HCe. The effect of the nanoparticles on CD3+T cells was evaluated by assaying proliferation rate, apoptosis and the release of IFN- γ , IL-17 and IL-10 both in unstimulated and lymphocytes stimulated by adding 0.15 mg/ml phytohemagglutinin (PHA). As controls, untreated cells and cells treated with everolimus (0.003 μ g/ml) in the same experimental conditions used for nanoparticles treatment were used, as previously described (Cova et al.,

2015). Long-time effect of nanoparticle incubation on lymphocytes viability was also assessed at 7 and 10 d after treatment. For these experiments, only PHA-treated cells were considered since it is widely known that unstimulated lymphocyte survival is limited to 48 h. Uptake of GNP-HC and GNP-PEG labeled with AF488 by macrophages, neutrophils and lymphocytes was evaluated after 2 h incubation at 37 °C in the complete medium by flow cytometry.

IL-8, IFN-g, IL-17, IL-10 and elastase detection

IL-8 production by unstimulated or stimulated (LPS treatment for 24 h) macrophages was evaluated by ELISA. The activation of neutrophils was assayed by the elastase release (enzymatic assay). Briefly, 2×10^7 isolated neutrophils were treated with 5 µg/ml cytochalasin B (Sigma-Aldrich, Milan, Italy) for 10 min at room temperature. Afterwards, cells were seeded in 96-well plate and treated for 20 min at 37 °C with different stimuli (nanoparticles or *N*-formyl-L-methionyl-L-leucyl-L-phenylalanine (FMLP, 10^{-4} M), as a positive control). After centrifugation (1000 g for 10 min at 4 °C) supernatants were added to a substrate solution (*N*-succinyl-Ala-Ala-p-nitroanilide, 1 mM in phosphate buffer), incubated for 1 h at 37 °C and read at 405 nm spectrophotometer beam. The data were expressed as % vs. untreated neutrophils. IFN-g detection was evaluated at 24 h after incubation while IL-10 and IL-17 dosage was performed after 48 h. IFN-g, IL-17 and IL-10 production was evaluated by ELISPOT procedure, as previously described (Bianco et al., 2005).

Cell proliferation, viability and apoptosis evaluation

Proliferation and apoptosis rate were evaluated by carboxyfluorescein succinimidyl ester (BD Pharmingen, Milan, Italy) and Annexin V (Molecular Probes, Life Technologies, Milan, Italy) by flow cytometry. Lymphocyte proliferation and apoptosis were evaluated at 24, 48 and 72 h while only apoptosis was considered for long time experiments (7 and 10 d after treatments). Neutrophil apoptosis was assayed after 4 h incubation. Proliferation and apoptosis were expressed as a percentage of dividing and apoptotic cells, respectively. MTT (3-(4,5-dimethylthiazol-2-yl)-2,5-diphenyltetrazolium bromide) test (Sigma-Aldrich, Milan, Italy) was used to assay macrophage viability at 24, 48, 72 h and 7 and 10 d incubation and was expressed as a percentage of variation vs. untreated cells.

Reactive oxygen species (ROS) detection

ROS level was detected at t_0 (baseline) and after 4 h of incubation with nanoparticles for neutrophils or 48 h for macrophages by electron paramagnetic resonance (EPR) spectroscopy (Bruker, Germany) operating at the common X-Band microwave frequency (~9.8 GHz). For ROS trapping, culture medium and cells were incubated with 1 mM CMH (1-hydroxy-3-methoxycarbonyl-2,2,5,5-tetramethylpyrrolidine) probe prepared in Krebs-Hepes buffer containing 25 µM deferoxamine methanesulfonate salt chelating agent and 5 µM sodium diethyldithiocarbamate trihydrate at pH 7.4 (Faoro et al., 2011). Spectra were recorded and analyzed by using a standard software (Win EPR version 2.11). Neutrophils and macrophages were re-suspended in 250 µl of CMH probe (1:1) and incubated for 30 min at 37 °C. Afterwards, samples were frozen at 77°K before acquisition by EPR (Mrakic-Spota et al., 2012).

Mitochondrial membrane potential assessment

Mitochondrial membrane potential (mtMP) was assessed by the JC-1 tracker. The ratio of the fluorescent intensity of J-aggregates

to fluorescent intensity of monomers was used as an indicator of cell health. Neutrophils and macrophages were plated at a density of 1×10^5 in 96-well black plates and incubated with GNP-HC and GNP-HCe for 4 and 48 h, respectively; at the end of treatment 10 µl of JC-1 staining solution (JC-1 reagent diluted 1:10 in culture medium) were added to the cells. After rinsing, the plates were read using a fluorescent plate reader (Fluostar Omega, BMG Labtech GmbH, Ortenberg, Germany).

CD3 + CD4+, CD3 + CD8 + populations and CCR7 expression

CD3 + lymphocytes were incubated with nanoparticles for 48 h and immunodecorated with mAbs against CD8, CD3, CD4 and CCR7 (Beckman Coulter, Milan, Italy) according to the manufacturer's instructions. The mAb were labeled with the fluorescent dyes PE-Texas Red, fluorescein isothiocyanate, allophycocyanin and phycoerythrin (PE), respectively. Cells were analyzed by an FACScan flow cytometer (Beckman Coulter).

Animal experiments

This study was conducted under EU guidelines for the care and use of laboratory animals in accordance with Italian and European legislation (D.lgs. 116/92, European Directives 86/609/EE for the protection of animals used in scientific and experimental studies and 2010-63UE) and was approved by Ethical Committee recognized from University of Pavia. Twenty-two C57/BL6 mice were purchased from Charles River (Charles River laboratories, Lecco, Italy) and housed in polycarbonate cages for 10 d after arrival. Inhaled mice were treated in a home-made chamber in which nanoparticles in suspension were administered by a commercial aerosol machine. Mice were divided into four groups: (1) three mice living in normal conditions for 3 d and 4 mice living in normal conditions for 2 weeks; (2) four mice subjected to aerosol treatment for 3 d, 30 min/day, with 50 µg/mouse of GNP-HCe; (3) eight mice subjected to aerosol treatment for 2 weeks, 5 d/week, 30 min/day, with 50 µg/mouse of GNP-HCe (4 mice) or GNP-HC (4 mice); (4) three mice subjected to an aerosol treatment for 2 weeks, 5 d/week, 30 min/day, with 50 µg/mouse of GNP-HC marked with IR-820 dye. For inhalation, nanoparticles were suspended in phosphate buffer. Immediately after the last inhalation, mice were anesthetized with intraperitoneal injection of 0.5 mg/g of Avertin (2, 2, 2-Tribromoethanol) and were sacrificed by cervical dislocation. The dose of nanoparticles administered to mice by inhalation (50 µg/mice/30 min inhalation) was chosen according to the *in vitro* data in which we selected 25 µg/ml as the more effective concentration and taking in account mice lung volume (Supplementary Table 1).

Bronchoalveolar lavage and IL-8 dosage

Third group and control mice were subjected to BAL after anesthesia and before sacrifice to measure IL-8 production by ELISA and to determine differential cell count by optical microscopy. BAL fluid was collected by using two consecutive instillations of PBS (1 ml) at room temperature and was centrifuged at 1500 rpm at 4° C for 10 min; supernatants were collected and stored at -80° C for measurement of IL-8 levels. Cell pellets were re-suspended in 100 µl PBS and cytospin samples stained with Papanicolaou dye for the differential cell count that were expressed as a percentage of macrophages, neutrophils and lymphocytes.

Histological examination of mice tissues

Paraffin-embedded sections of 5 µm of lungs, spleen, kidneys and liver isolated from control mice or mice treated for 2 weeks with

GNP-HC and GNP-HCe were stained with hematoxylin and eosin for evaluation. For lungs, the degree of alveolar congestion, hemorrhage, leukocyte infiltration and the thickness of the alveolar wall were assessed. For liver, we examined the presence of alterations in the architecture, in the hepatocytes, in portal triads and sinusoids, inflammation and degeneration, Kupffer cells hyperplasia, necrosis, fatty impairment and portal fibrosis. For kidneys, we observed proximal and distal tubules, glomerular network, the volume of capsules in renal corpuscle, inflammation and fibrosis. For spleen, the degree of congestion of red pulp, inflammation, fibrosis and widening sinusoids were evaluated.

Near infrared light microscopy (NIR) technology

After sacrifice, mice treated for 2 weeks with IR820 dye-NH₂ labeled GNP-HC were perfused with cold PBS and then with 4% paraformaldehyde solution. Lungs, liver, spleen and kidneys were removed and left for 24 h in paraformaldehyde. For relative quantification of signal intensity, images were obtained using the Odyssey[®] Infrared Imaging System (LI-COR Biosciences, Lincoln, NE). Briefly, isolated organs were placed on the surface of the image and high-resolution scans were performed with the following parameters: near-infrared 700 and near-infrared 800 scan intensity 3, resolution 21 μ m, and focus 2.5 mm. For quantitative evaluation, five regions of interest were traced in the organs, and near-infrared 700 signal intensity values were recorded using Odyssey[®] software.

Gold quantification by ICP-OES analysis

For ICP-OES analysis, samples from liver, spleen and kidney of untreated mice and mice treated for 2 weeks were diluted with aqua regia to a maximum of 3 ml and left 72 h. Next, samples were further diluted to 10 ml adding distilled water. All samples were measured in triplicate with Optima 7000 DV ICP-OES (PerkinElmer, Waltham, MA).

Transmission electron microscopy

Samples obtained from lungs of mice treated for 3 d or 2 weeks with GNP-HC or GNP-HCe were fixed by 2.5% glutaraldehyde in PBS. After three washes with the same buffer, the samples were postfixed for 2 h with 1.5% osmium tetroxide in PBS, dehydrated by a rising alcohol scale and included in epoxin resin. Ultrathin slices (70/80 nm) were cut and dyed with uranyl acetate and citrate lead.

Statistical analysis

Statistical differences between untreated cells, cells treated with different nanoparticles and everolimus alone were evaluated using ANOVA analysis. All analyses were carried out with Graph Prism 5.0 statistical program (GraphPad Prism, San Diego, CA). A *p* value <0.05 was considered statistically significant.

Results

Effect of nanoparticles on macrophage activation

Experiments performed with dye-labeled nanoparticles showed that macrophages were able to incorporate both GNP-PEG and GNP-HC nanoparticles (Supplementary Figure 1A) according to the phagocytic nature of these cells. Under unstimulated conditions (Figure 1(A)), we observed that GNP-HCe significantly decreased

the metabolic activity of macrophages after 72 h of treatment compared to everolimus alone and GNP-HC, suggesting that everolimus inside GNPs exerted an anti-inflammatory activity in unstimulated macrophages. Under LPS stimulation (Figure 1(A)), GNP-HCe slightly decreased macrophage viability, but with no significant differences with respect to everolimus alone. Long-time exposure to CD44-decorated nanoparticles with everolimus resulted in significantly affected viability either in normal or LPS-stimulated macrophages compared to the slightly less impairment observed in the presence of everolimus alone (Supplementary Figure 4A). As a control, we assessed the effect of GNP-PEG and GNP-PEGe on macrophages and found a significantly reduced cell viability only in the presence of GNP-PEGe due to a release of the drug inside the cells (Supplementary Figure 1A). IL-8 production by LPS-stimulated and unstimulated macrophages was not significantly changed by the treatment with all the nanoparticles used (Figure 1(B) and Supplementary Figure 1B) also after long time exposure (Supplementary Figure 4B). Since no significant cell activation was induced by GNP-PEG and GNP-PEGe the following experiments were performed only with antibody-engineered nanovectors. The impairment of cell viability by GNP-HCe both in LPS-treated and untreated macrophages was confirmed by measurements of the mtMP, as shown by the remarkable decrease in red/green intensity ratio of JC-1 (Figure 1(E)). When assessing GNP-HC toxicity by MTT and JC-1 tests, we did not obtain comparable results. We hypothesized that JC-1 assay sensitivity was much higher compared to MTT in our experiments, although further investigation are underway to elucidate such discrepancy. As a possible sign of activation induced by nanoparticles, we also evaluated the production of ROS, as it represents a defense mechanism characteristic of phagocytes. Unstimulated cells showed a slight but significant increase in extracellular ROS production with GNP-HCe but it seemed more a release from intracellular compartment instead of a novel burst (Figure 1(C)). On the other hand, in the case of LPS-stimulated macrophages, GNP-HCe did not stimulate intracellular and extracellular ROS production. This is an important point because the ROS release by macrophages enhances the recruitment of inflammatory effectors at the site of injury, prolonging a profibrotic inflammatory response (Wynn, 2011). In our experimental conditions, the incubation with everolimus significantly increased ROS secretion in LPS-stimulated cells while GNP-HCe and GNP-HC did not. This difference could be assigned to the presence of anti-CD44 antibody on GNP surface since an involvement of CD44 in ROS defense pathway has been documented (Ishimoto et al., 2014).

Effect of nanoparticles on neutrophil activation

Flow cytometry experiments showed that polymorphonuclear cells (PMNs) were able to uptake both GNP-PEG and GNP-HC nanoparticles (Supplementary Figure 1B) given their phagocytic nature associated to the key microbicidal function of innate immunity cells (Lee et al., 2003). PMNs have a very short half-life (6–8 h), which is even shorter when they are stimulated (Summers et al., 2010). For this reason, we could only analyze the effects of GNP-HCe under basal condition as soon as they were isolated from peripheral blood, using as a positive control neutrophils stimulated with FMLP, a naturally occurring bacterial peptide that stimulates PMNs through a specific membrane receptor (Torres et al., 1993). Both GNP-HC and GNP-HCe did not affect elastase release (Figure 2(A)). Only a slight increase in apoptotic rate was induced by GNP-HCe compared to untreated neutrophils or neutrophils incubated with GNP-HC or everolimus alone (Figure 2(B)). Since we proved that unfunctionalized nanoparticles with or without

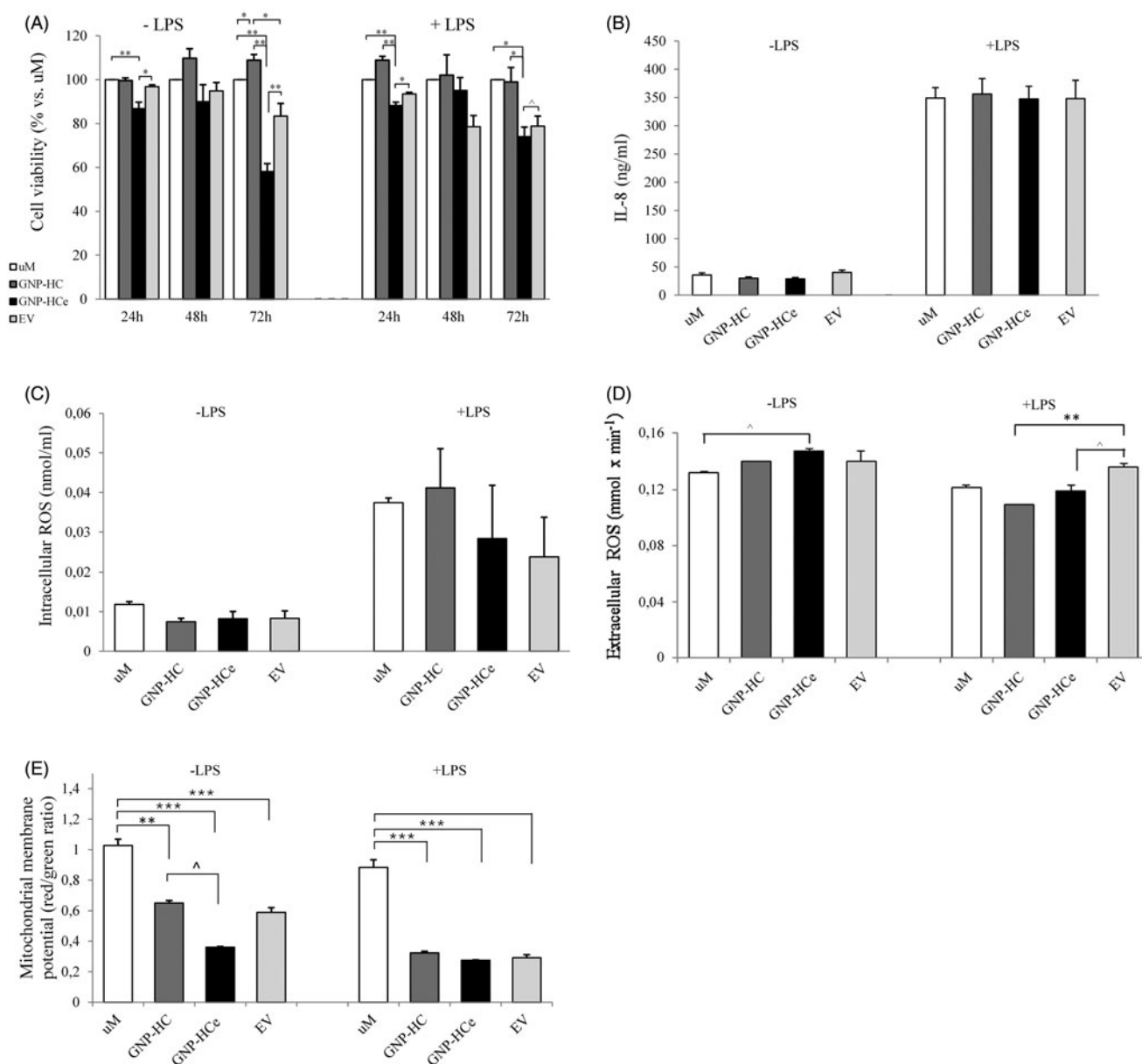


Figure 1. Effect of nanoparticles on macrophage activation. (A) Cell viability assayed at 24, 48 and 72 h after 2 h incubation. (B) IL-8 secretion by LPS-stimulated and unstimulated macrophages. (C) Intracellular and (D) extracellular ROS level evaluated at 48 h after 2 h incubation. (E) Mitochondrial membrane potential after 48 h incubation. Histograms are obtained from the means \pm standard error of three experiments. *** $p < 0.0001$; ** $p < 0.001$; * $p < 0.01$; $\wedge p < 0.05$. uM: untreated macrophages; LPS: lipopolysaccharides.

everolimus, GNP-PEGe and GNP-PEG, respectively, did not affect PMNs activity (Supplementary Figure 2C), the following experiments were performed only with decorated GNPs. GNP-HCe and everolimus alone significantly increased ROS production in culture media with a concomitant marked a drop in intracellular free radicals suggesting a leakage of ROS from the cells rather than a burst (Figure 2(C) and (D)). In analogy to macrophages, the mtMP of PMNs was significantly affected by both GNP-HC and GNP-HCe while no changes were induced by incubation with everolimus (Figure 2(E)).

Effect of nanoparticles on lymphocyte activation

In preliminary experiments, we confirmed previous data on lymphocyte expression of CD44 (Baaten et al., 2010; Guan et al., 2011). Since only Ab-decorated nanoparticles were internalized by cells (Supplementary Figure 1C), lymphocyte incubation was

performed using GNP-HC and GNP-HCe. Experiments were carried out with unstimulated and stimulated (PHA mitogen stimulation) T lymphocytes. No differences in proliferation rate were recorded in basal or PHA-stimulated cells treated with GNP-HC and GNP-HCe (Supplementary Figure 3). The differentiation of lymphocytes is regulated by proliferation, migration and also by cell death. In particular, activation-induced cell death (AICD) in T cells plays a pivotal role in maintaining self-tolerance after transplantation (Nakano et al., 2007; Russell, 1995). For this reason, we decided to analyze the impact of GNP-HCe on the apoptosis rate of activated lymphocytes, as well as under basal conditions, to assess the potential of our nanoconstruct to ameliorate tolerance toward graft through the induction of T cell apoptosis. Treatment of PHA-stimulated cells with GNP-HCe resulted in significant increase in apoptotic rate after 8 h, which protracted after 24 h, as compared to everolimus alone, whose effect vanished with time (Figure 3(A)). These results indicate a persisting action of the drug as a result of a long-lasting

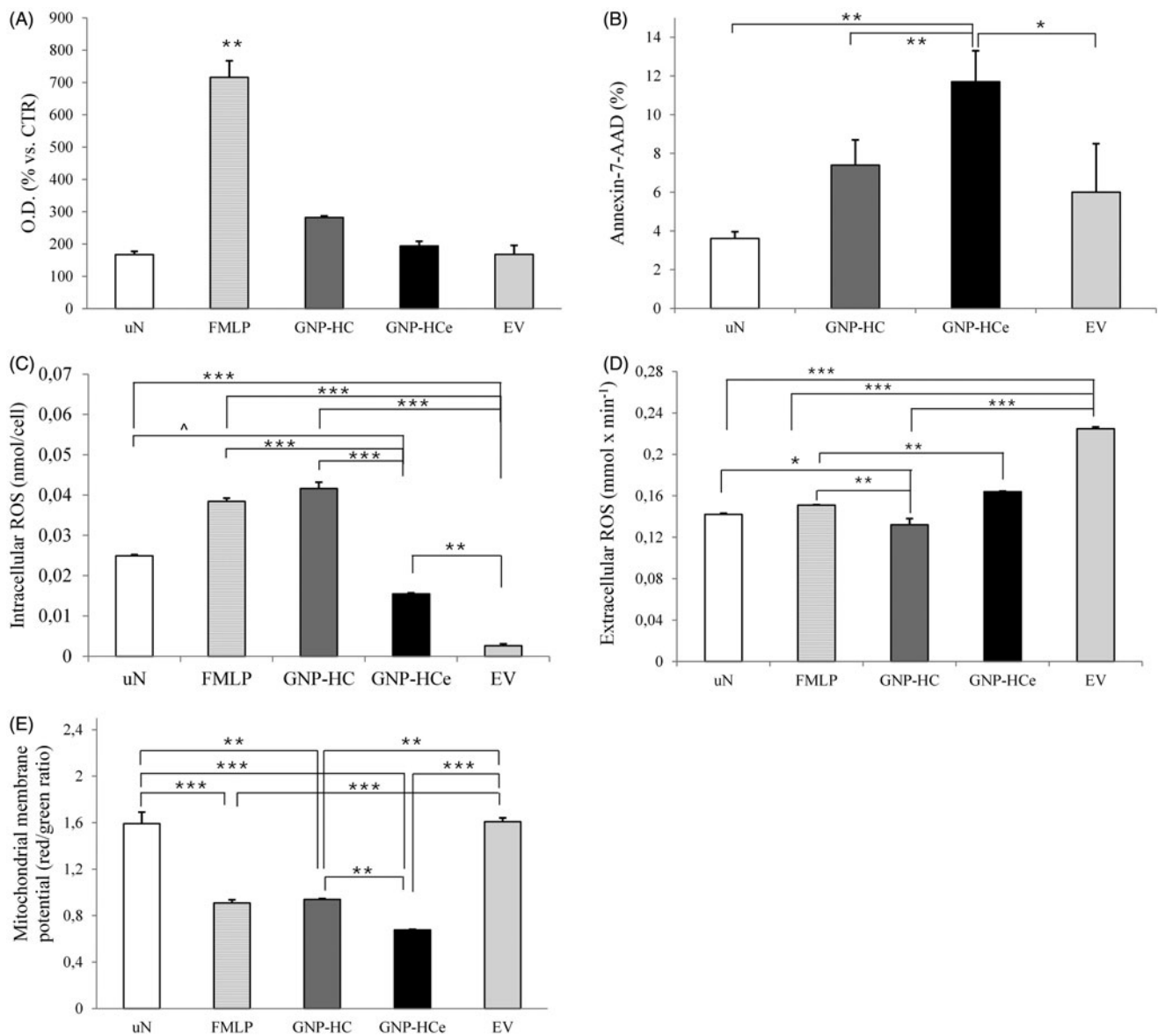


Figure 2. Effect of nanoparticles on neutrophil activation. (A) Elastase secretion. Neutrophil responsiveness was proved by elastase secretion induced by FMLP. (B) Apoptotic rate and cell death. (C) Intracellular and (D) extracellular ROS level evaluated after 2h incubation. (E) Mitochondrial membrane potential. Histograms are obtained from the means \pm standard error of three experiments. *** $p < 0.0001$; ** $p < 0.001$; * $p < 0.01$; $\wedge p < 0.05$. uN: untreated neutrophils; FMLP: positive control.

intracellular release. It is worth noting that GNP-HC and GNP-HCe exerted a comparable effect especially under basal conditions (Figure 3(A)). The improved effect of everolimus formulated via GNP compared to the drug alone was particularly evident in the analysis of cytokine production by PHA-stimulated T cells since GNP-HCe significantly decreased INF- γ , IL-17 and IL-10 secretion compared to everolimus alone, which, in contrast, had no effect (Figure 3(B)). After 7 and 10 d of exposure to CD44-decorated nanoparticles and everolimus alone lymphocytes showed a massive apoptosis suggesting that also long-exposure exert an anti-inflammatory effect (Supplementary Figure 4C).

MTOR has many different activities, among which the capability to affect the regulation of T cell trafficking by modulating CD8⁺ and CD4⁺ expression as well as the rate of CCR7 on T cells (Araki et al., 2011). Consequently, inhibition of mTOR by rapamycin or by its derivative everolimus modulates CD8⁺ and CD4⁺ differentiation and expression. Therefore, we assayed the *in vitro* effect of

GNP-HCe on CD4⁺ and CD8⁺ expression in CD3⁺ lymphocytes population in order to evaluate whether and how everolimus delivered by GNP could modulate the expression of these two receptors over time, as compared to the free drug. We found that GNP-HCe slightly reduced the CD3⁺CD4⁺ population under both experimental conditions (\pm PHA) similarly to everolimus alone (Figure 3(C)) after 48 h incubation. As for CD3⁺CD8⁺ population, the effect of everolimus was evident only if the drug was incorporated in GNP (Figure 3(D)). Moreover, also in this case, GNP-HC showed a similar effect as GNP-HCe. In addition, it is known that inhibitors of mTOR increase the expression of CCR7, a chemokine receptor necessary for T-cells exit from peripheral tissues (Araki et al., 2011; Debes et al., 2005). We observed that the expression of CCR7 on both CD4⁺ and CD8⁺ cells was significantly increased over a 48 h treatment only with GNP encapsulated with the drug, while the effect of everolimus alone was much weaker (Figure 3(E) and (F)).

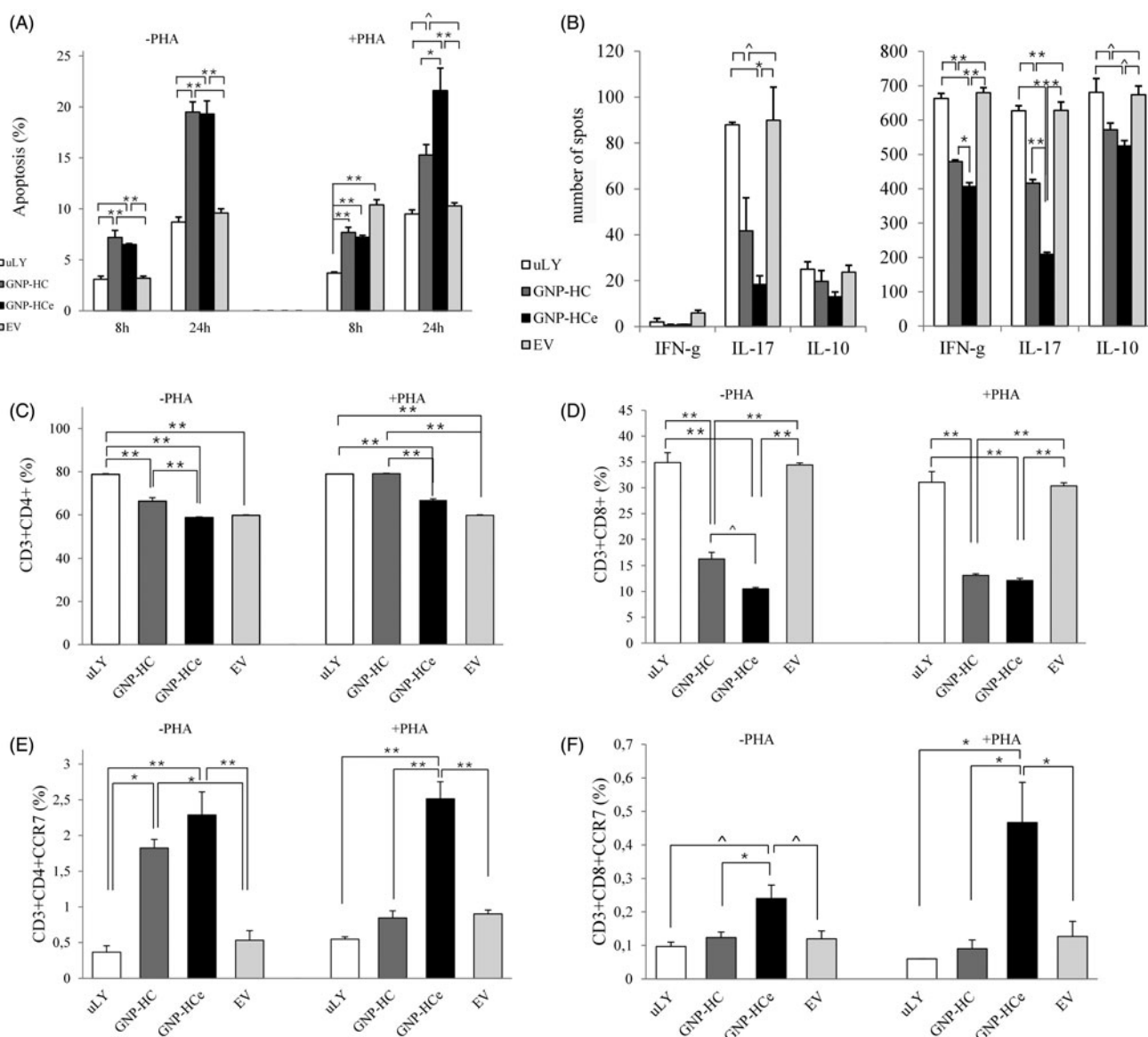


Figure 3. Effect of nanoparticles on lymphocyte activation. (A) Apoptosis evaluated at 8 and 24 h after 2 h incubation in unstimulated and PHA-stimulated lymphocytes. (B) IFN-g, IL-17 and IL-10 secretion in un-stimulated and PHA-stimulated lymphocytes. Cytokine production is expressed as a number of positive spots/ 1.5×10^5 cells for IFN-g and 3×10^5 cells for IL-17 and IL-10. (C) CD4+ and (D) CD8+ expression in unstimulated and PHA-stimulated conditions. (E, F) The CCR7 expression on CD4+ and CD8+. Histograms are obtained from the means \pm standard error of three experiments. *** $p < 0.0001$; ** $p < 0.001$; * $p < 0.01$; $\wedge p < 0.05$. uLy: untreated lymphocytes; PHA: phytohemagglutinin.

Localization and effect of inhaled nanoparticles in normal mice

One of the main objectives, when we designed the nanovehicle-based treatment to specifically target MCs, was to administer them by the inhalatory route. Therefore, we undertook *in vivo* experiments treating normal mice with: a) fluorescent-marked GNP-HC without everolimus to understand the fate of NPs and b) GNP-HCe in order to evaluate if our “fully armed” GNPs could induce an inflammatory insult. NIR technology demonstrated that mice lungs were strongly positive to fluorescence marker when inhaled with IR820-labeled GNP-HC (Figure 4(B) and (C)) compared to untreated mice (Figure 4(A)). Instead, no signal differences were recorded in liver, kidney and spleen between inhaled and control mice (Figure 4(C)). ICP experiments confirmed that gold amount in liver (in percentage, mean \pm SD: 105.5 ± 0.34), spleen (in percentage, mean \pm SD: 118.3 ± 13.9) and kidney (in percentage, mean \pm SD: 101.6 ± 12.9) was not significantly different from that found in the respective organs of untreated mice (reference

value, 100%). Neither significant induction of IL-8 production in BAL of mice inhaled for 2 weeks with functionalized nanoparticles with or without everolimus inside (Figure 4(D)) nor an increased recruitment of macrophages, neutrophils or lymphocytes in the bronchoalveolar lumen as reflected by unchanged BAL cellularity were observed (Supplementary Table 2). TEM showed that functionalized nanoparticles were localized in the bronchoalveolar lumen and on cell luminal surface of epithelial cells (Figure 5(A) and (B)). As expected (Alkilany & Murphy, 2010; Geiser et al., 2013; Gosens et al., 2010; Han et al., 2015; Sadauskas et al., 2009), nanoparticles were extensively taken up by alveolar phagocytes (Figure 5(C)). The same distribution was detected after 3 d inhalation although, according to a less exposure, a small amount of nanoparticles was present inside lung tissue (Supplementary Figure 5). Histological examination of liver, kidney and spleen slices evidenced no morphologic tissue alterations after a 15 d course of treatment either with GNP-HC or GNP-HCe.

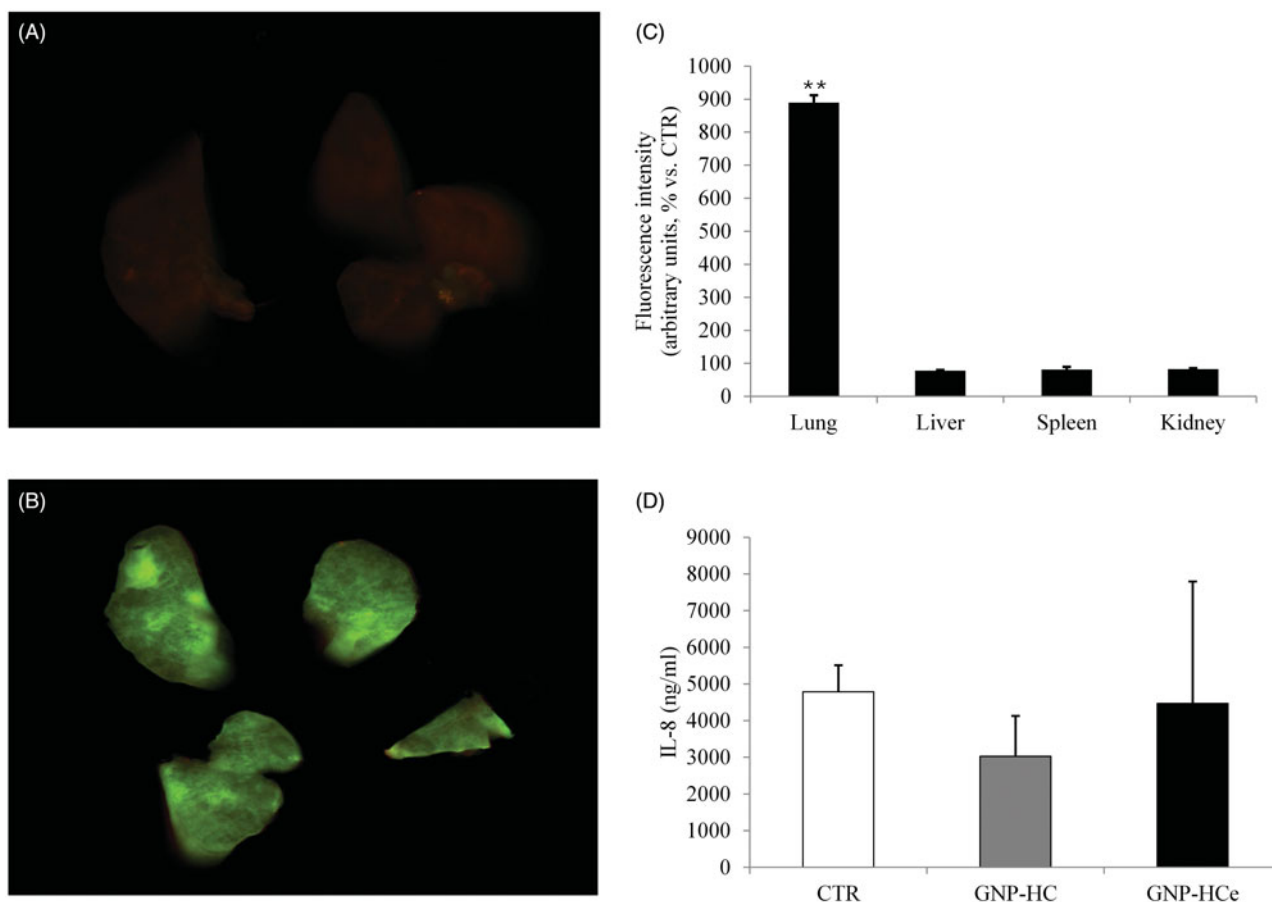


Figure 4. Localization of nanoparticles in lung and peripheral tissues and effect on IL-8 lung production. Representative experiment showing (A) un-treated and (B) treated lungs. A weak auto-fluorescence background (red) is detected in un-treated lungs (A) while lungs inhaled GNP-HC nanoparticles marked with IR-820 dye show a high fluorescence signal (green, B). Fluorescence intensity recorded in different organs (lung, liver, spleen and kidney) of mice inhaled GNP-HC nanoparticles marked with IR-820 dye is evaluated compared to the same organs of un-treated mice (C). IL-8 production assayed in BAL of un-treated and treated (GNP-HC and GNP-HCe) mice (D). Histograms are obtained from the means \pm standard error of three experiments. ** $p < 0.001$ vs. all other tissues.

Discussion

Among the renewed strategies allowed by the advent of nanomedicine, targeted drug delivery is particularly attractive in those pathologies for which the local and target treatment represents a chance to avoid excessive systemic toxicity and increase the therapeutic effectiveness. In this perspective, great attention has been devoted to GNPs that are considered “safe” and biocompatible material (Alkilany & Murphy, 2010; Shukla et al., 2005). With the aim to find out a new therapeutic strategy for CLAD, which affects about 50% of patients at 5 year after transplantation, we engineered GNPs loaded with an immune-suppressive/anti-proliferative drug specifically targeted against pulmonary MCs, the main effectors driving the fibroproliferative obliteration of bronchioles. In the previous work (Cova et al., 2015), we proved the *in vitro* efficacy of these nanoparticles to inhibit MC without affecting the viability of bronchoalveolar epithelial cells. The pathogenesis of BOS is though as a multistep process including a primary damage to the epithelia, followed by chronic airway inflammation which ultimately arouses the recruitment and proliferation of mesenchymal effectors and airway fibro-obliteration. For this reason, inflammatory cells, alveolar macrophages, neutrophils and lymphocytes play a primary role in establishing the reactive local milieu that promotes fibrosis. Thus, it is mandatory to exclude a proinflammatory activity of our GNPs.

In this work, we performed the experiments *in vitro* either using unstimulated isolated cells and after a proper stimulation,

the latter condition mimicking an already activated/inflamed environment, thus covering the different physiological conditions in which the future *in vivo* nanoparticle administration could play their activity. As for macrophages, no stimulatory effect or increased oxidative stress was observed by treatment with GNPs decorated with the antibody either under basal or activated conditions, as previously described for gold nanocarriers (undecorated GNPs) (Shukla et al., 2005). In contrast, a reduced macrophage viability was recorded with GNPs loaded with everolimus (either coated or not with anti CD44), demonstrating that the toxic effect was actually due to the drug release into the phagocytes. Also, long-term experiments proved the superiority of the treatment with drug-loaded nanoparticles in inhibiting macrophage viability compared to everolimus alone. Similar results were obtained with neutrophils. Thus, in analogy to previous findings (Uchiyama et al., 2014) we did not detect a significant pro or anti-inflammatory activity of “nude” GNPs, but we found that functionalized or functionalized and drug loaded ones were able to partially downregulate phagocytic activities. A considerably higher inhibitory activity of GNP-HCe was detectable toward lymphocytes, in particular, IFN-g and IL-17 secretion by stimulated T cells, was markedly downregulated. This result is particularly relevant in the perspective of future therapies based on GNP-HCe, because IFN-g and IL-17 are two key cytokines in BOS pathogenesis. In particular, IFN-g mostly produced by activated T cells is a major player in allograft rejection in that induces major histocompatibility complex expression in epithelial and endothelial cells against foreign

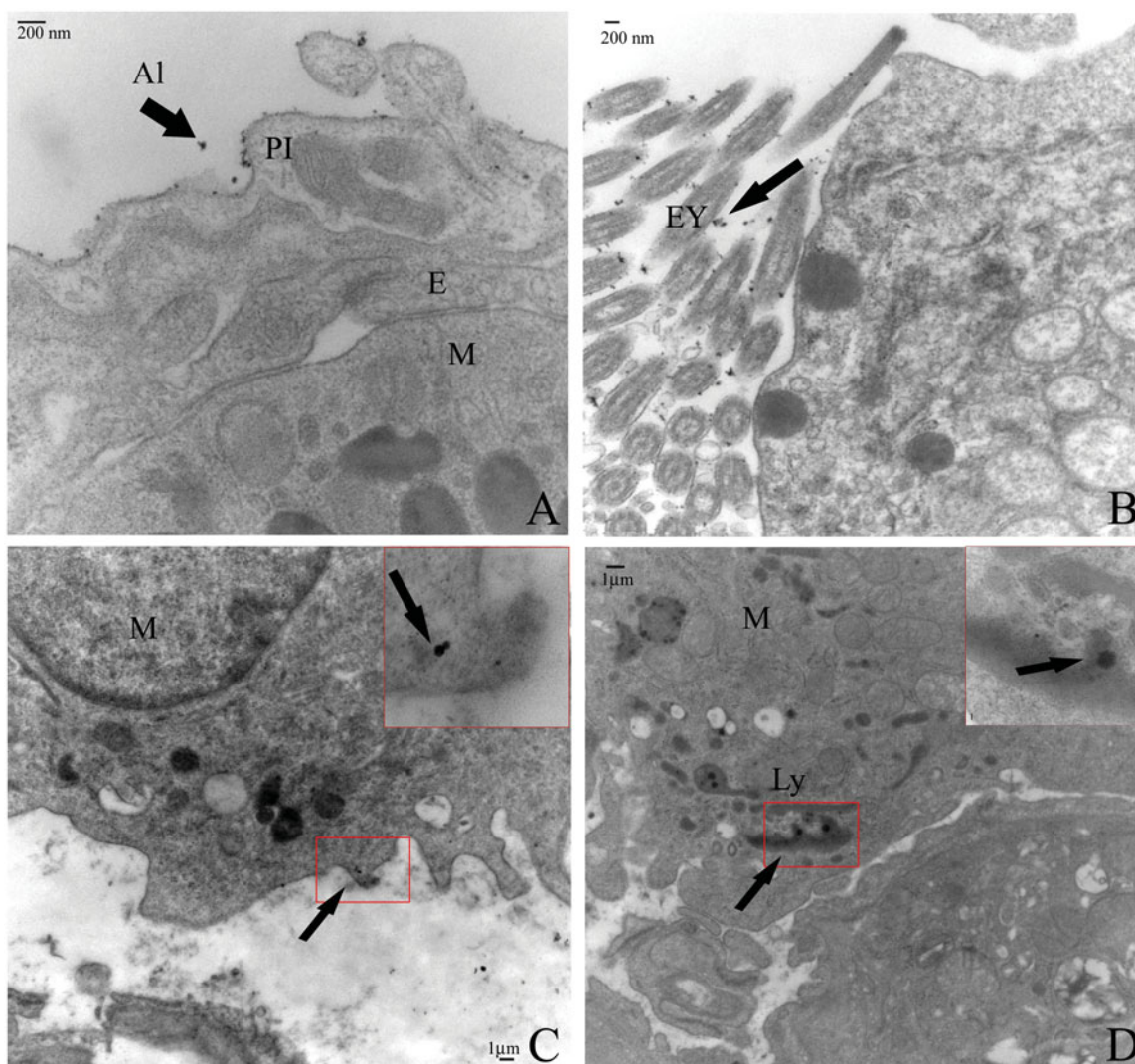


Figure 5. Subcellular localization of functionalized nanoparticles in inhaled lungs. (A, B) Transmission electron microscopy images of GNP-HC (indicated by arrows) localization in the bronchoalveolar lumen and on the surface of pneumocytes. (C) Positive intracellular and (D) intra-lysosome signal in alveolar macrophages with a particular of the same picture a higher magnification (inserts). M: macrophages; PI: pneumocytes; E: endothelium; EY: lung eyelashes; Al: alveolus; LY: lysosome.

antigens (Halloran et al., 2001; Hidalgo & Halloran, 2002). Furthermore, IL-17 is a potent inducer of IL-8 release by lung endothelial and epithelial cells, creating a chemotactic gradient toward airways lumen for innate immune cells (Elssner & Vogelmeier, 2001; Palmer et al., 2005; Vanaudenaerde et al., 2011). In addition, previous evidence showed that the mTOR inhibitors and, in general, drugs derived from rapamycin (TOR) (Araki et al., 2011) regulate differentiation and trafficking of lymphocyte subsets. Our results showing a reduction of the percentage of CD4⁺ and CD8⁺T cells, together with a decreased CCR7 expression, suggest that GNP-HCe could improve the propensity of these cells to home to secondary lymphoid tissues, reducing their traffic to site of inflammation, thus ultimately promoting allograft survival (Araki et al., 2011).

Our study provided also an unexpected finding, the observation that also GNP-HC exerted a significant inhibitory activity on T cells suggesting that the interaction of the anti-CD44 antibody with a CD44 receptor on lymphocytes might induce *per se* an apoptotic signaling pathway in lymphocytes. Several researchers investigated the role of CD44 in the regulation of AICD in T cells, but there is not a general consensus on its effect, probably due to the difference in methodologies (different T cell subsets, various

antibody-mediated CD44 ligation) (Baaten et al., 2010). Our results seem to suggest that anti-CD44 targeting might enhance the activity of everolimus thus possibly leading to an enhancement of graft tolerance.

After the achievement of these encouraging *in vitro* data showing the lack of a proinflammatory activity of our engineered GNPs, we moved to assess the *in vivo* localization and toxicity. Our results confirmed that inhaled nanoparticles did not rise the inflammatory response at the pulmonary level, did not even induce significant toxicity and seemingly localized mainly into alveolar space due to capture by macrophages. It has to be noted that our delivery schedule included 30-min inhalation a day for up to 2 weeks. In another work, a single intratracheal instillation of 50 and 250 nm GNPs generated only a mild inflammatory response that was mostly localized in alveolar macrophages (Gosens et al., 2010). The absence of inflammatory response observed by us in lung tissues could be ascribed to the different administration procedure since instillation results in the acute delivery of a higher nanoparticle load than inhalation by aerosolization usually associated with a higher dispersion rate. TEM images showed that anti-CD44 mAb-functionalized GNPs were not present as agglomerates and resided prevalently into alveolar

macrophages, suggesting that macrophage clearance could represent the prominent defense line and accumulation site of these nanotools (Balasubramanian et al., 2013). This observation together with the lack of fluorescence and gold signal in peripheral tissues, is in agreement with previous reports in which GNPs with similar size locally administered by inhalation or intratracheal instillation were mostly retained in the lungs (Balasubramanian et al., 2013; Geiser et al., 2013; Gosens et al., 2010; Han et al., 2015; Kreyling et al., 2014; Sadauskas et al., 2009; Sung et al., 2011). In two different studies, for example, the authors found an accumulation of GNPs in the kidneys and the liver, respectively (Sung et al., 2011; Yu et al., 2009). However, inhalation was performed, in the first case, for longer time (90 d) while, in the second study, smaller nanoparticles (20 nm) were used. The final destination of colloidal nanoparticles administered *in vivo* is often strictly associated to the physical–chemical properties of the outer polymer (Alkilany & Murphy, 2010; Niidome et al., 2006; Yu et al., 2009). In this light, another important breakthrough of our study is represented by the coating that has been used for stabilizing and functionalizing our GNPs, since the peculiar amphiphilic character of PMA (Fiandra et al., 2013; Lin et al., 2008) proved to be particularly suitable to promote the transepithelial penetration of nanoparticles, their interaction with target cells and diffusion into the cytoplasm, allowing the drug to be released directly in the compartment in which it can exert its functional activity.

In our protocol, mice are treated for a short time (i.e. 20 weeks), while subchronic treatments, usually requiring at least 28–90 d treatment, would be more exhaustive to evaluate possible long-term toxic effects of GNP-HC and of GNP-HCe. However, we agree with Han et al. (2015) that subchronic treatment is expensive and time-consuming at least in these experiments finalized to set up inhalation conditions, nanoparticles localization, rough toxicity and approximate dose. In fact, we proved that the *in vivo* inhalation of aerosolized GNPs resulted in a consistent accumulation of functionalized nanoparticles at the target organ. This result was somewhat unexpected since both inhalation conditions and dose amount were set on assumed calculations and home-made chamber that should mimic an inhalatory device for patients' administration. Future experiments will be performed on BOS animal models in order to assess the efficacy of GNP-HCe in preventing/reverting chronic rejection considering that nanoparticles uptake and behavior might be different in diseased lungs, as previously described (Geiser et al., 2013).

Conclusion

The use of nanoparticles in the attempt to solve urgent medical need represents a huge challenge and this work discloses the possibility to extend the use of this innovative tool to prevent/revert the onset of chronic rejection after lung transplantation, namely BOS. Here, we prove that our nanoparticles specifically functionalized with an antibody directed against lung MCs BOS patients, do not stimulate inflammatory cells. Although these are *in vitro* observations, they confirm the potential validity in the treatment of BOS since they do not elicit an inflammatory response. *In vivo* experiments comply with *in vitro* observations and, demonstrating the feasibility of the local inhalatory administration route, allow us to rationalize the dose schedule and the number of animals to be used in future experiments aimed to assess therapeutic activity in BOS models. The results of our study confirm that this drug-loaded engineered nanoconstruct is able to exert its therapeutic action without enhancing the activity of immune effectors thus leaving the inflammatory response and oxidative stress essentially

unaltered, with positive implications on the translational potential of this therapeutic strategy.

Acknowledgements

We thank Dr. Silvia Cerri for her helpful assistance in NIR experiments and Dr. Fabio Blandini for the opportunity to use the Odyssey[®] Infrared Imaging System.

Disclosure statement

The authors report no conflicts of interest. The authors alone are responsible for the content and writing of this article.

Funding

This work was supported by Fondazione Cariplo [grant no. 2013-0943].

References

- Alkilany AM, Murphy CJ. 2010. Toxicity and cellular uptake of gold nanoparticles: what we have learned so far? *J Nanopart Res* 12:2313–33.
- Araki K, Ellebedy AH, Ahmed R. 2011. TOR in the immune system. *Curr Opin Cell Biol* 23:707–15.
- Baaten BJ, Li CR, Bradley LM. 2010. Multifaceted regulation of T cells by CD44. *Commun Integr Biol* 3:508–12.
- Badri L, Murray S, Liu LX, Walker NM, Flint A, Wadhwa A, et al. 2011. Mesenchymal stromal cells in bronchoalveolar lavage as predictors of bronchiolitis obliterans syndrome. *Am J Respir Crit Care Med* 183:1062–70.
- Balasubramanian SK, Poh KW, Ong CN, Kreyling WG, Ong WY, Yu LE. 2013. The effect of primary particle size on biodistribution of inhaled gold nano-agglomerates. *Biomaterials* 34:5439–52.
- Bianco AM, Solari N, Miserere S, Pellegrini C, Vitulo P, Pozzi E, et al. 2005. The frequency of interleukin-10- and interleukin-5-secreting CD4+ T cells correlates to tolerance of transplanted lung. *Transplant Proc* 37:2255–6.
- Biju V, Itoh T, Anas A, Sujith A, Ishikawa M. 2008. Semiconductor quantum dots and metal nanoparticles: syntheses, optical properties, and biological applications. *Anal Bioanal Chem* 391:2469–95.
- Brust M, Walker M, Bethell D, Schriffin DJ, Whymann RJ. 1994. Synthesis of thiol-derivatized gold nanoparticles in a two phase liquid-liquid system. *Chem Commun* 7:801–4.
- Cole LE, Ross RD, Tilley JM, Vargo-Gogola T, Roeder RK. 2015. Gold nanoparticles as contrast agents in x-ray imaging and computed tomography. *Nanomedicine (Lond)* 10:321–41.
- Cooper DR, Bekah D, Nadeau JL. 2014. Gold nanoparticles and their alternatives for radiation therapy enhancement. *Front Chem* 2:86.
- Cova E, Colombo M, Inghilleri S, Morosini M, Miserere S, Penaranda-Avila J, et al. 2015. Antibody-engineered nanoparticles selectively inhibit mesenchymal cells isolated from patients with chronic lung allograft dysfunction. *Nanomedicine (Lond)* 10:9–23.
- Debes GF, Arnold CN, Young AJ, Krautwald S, Lipp M, Hay JB, Butcher EC. 2005. Chemokine receptor CCR7 required for T lymphocyte exit from peripheral tissues. *Nat Immunol* 6:889–94.
- El-Sayed IH, Huang X, El-Sayed MA. 2005. Surface plasmon resonance scattering and absorption of anti-EGFR antibody

- conjugated gold nanoparticles in cancer diagnostics: applications in oral cancer. *Nano Lett* 5:829–34.
- Ellsner A, Vogelmeier C. 2001. The role of neutrophils in the pathogenesis of obliterative bronchiolitis after lung transplantation. *Transpl Infect Dis* 3:168–76.
- Faoro V, Fink B, Taudorf S, Dehnert C, Berger MM, Swenson ER, et al. 2011. Acute *in vitro* hypoxia and high-altitude (4,559 m) exposure decreases leukocyte oxygen consumption. *Am J Physiol Regul Integr Comp Physiol* 300:R32–9.
- Fiandra L, Mazzucchelli S, De Palma C, Colombo M, Allevi R, Sommaruga S, et al. 2013. Assessing the *in vivo* targeting efficiency of multifunctional nanoconstructs bearing antibody-derived ligands. *ACS Nano* 7:6092–102.
- Geiser M, Quaille O, Wenk A, Wigge C, Eigeldinger-Berthou S, Hirn S, et al. 2013. Cellular uptake and localization of inhaled gold nanoparticles in lungs of mice with chronic obstructive pulmonary disease. *Part Fibre Toxicol* 10:19.
- Giljohann DA, Seferos DS, Daniel WL, Massich MD, Patel PC, Mirkin CA. 2010. Gold nanoparticles for biology and medicine. *Angew Chem Int Ed Engl* 49:3280–94.
- Gosens I, Post JA, de la Fonteyne LJ, Jansen EH, Geus JW, Cassee FR, de Jong WH. 2010. Impact of agglomeration state of nano- and submicron sized gold particles on pulmonary inflammation. *Part Fibre Toxicol* 7:37.
- Guan H, Nagarkatti PS, Nagarkatti M. 2011. CD44 reciprocally regulates the differentiation of encephalitogenic Th1/Th17 and Th2/regulatory T cells through epigenetic modulation involving DNA methylation of cytokine gene promoters, thereby controlling the development of experimental autoimmune encephalomyelitis. *J Immunol* 186:6955–64.
- Halloran PF, Afrouzian M, Ramassar V, Urmson J, Zhu LF, Helms LM, et al. 2001. Interferon-gamma acts directly on rejecting renal allografts to prevent graft necrosis. *Am J Pathol* 158:215–26.
- Han SG, Lee JS, Ahn K, Kim YS, Kim JK, Lee JH, et al. 2015. Size-dependent clearance of gold nanoparticles from lungs of Sprague–Dawley rats after short-term inhalation exposure. *Arch Toxicol* 89:1083–94.
- Hardison MT, Galin FS, Calderon CE, Djekic UV, Parker SB, Wille KM, et al. 2009. The presence of a matrix-derived neutrophil chemoattractant in bronchiolitis obliterans syndrome after lung transplantation. *J Immunol* 182:4423–31.
- Heo DN, Yang DH, Moon HJ, Lee JB, Bae MS, Lee SC, et al. 2012. Gold nanoparticles surface-functionalized with paclitaxel drug and biotin receptor as theranostic agents for cancer therapy. *Biomaterials* 33:856–66.
- Hidalgo LG, Halloran PF. 2002. Role of IFN-gamma in allograft rejection. *Crit Rev Immunol* 22:317–49.
- Ishimoto T, Sugihara H, Watanabe M, Sawayama H, Iwatsuki M, Baba Y, et al. 2014. Macrophage-derived reactive oxygen species suppress miR-328 targeting CD44 in cancer cells and promote redox adaptation. *Carcinogenesis* 35:1003–11.
- Khatwa UA, Kleibrink BE, Shapiro SD, Subramaniam M. 2010. MMP-8 promotes polymorphonuclear cell migration through collagen barriers in obliterative bronchiolitis. *J Leukoc Biol* 87:69–77.
- Kreyling WG, Hirn S, Moller W, Schleh C, Wenk A, Celik G, et al. 2014. Air-blood barrier translocation of tracheally instilled gold nanoparticles inversely depends on particle size. *ACS Nano* 8:222–33.
- Lee WL, Harrison RE, Grinstein S. 2003. Phagocytosis by neutrophils. *Microbes Infect* 5:1299–306.
- Lin CA, Sperling RA, Li JK, Yang TY, Li PY, Zanella M, et al. 2008. Design of an amphiphilic polymer for nanoparticle coating and functionalization. *Small* 4:334–41.
- Liu A, Ye B. 2013. Application of gold nanoparticles in biomedical researches and diagnosis. *Clin Lab* 59:23–36.
- Mieszawska AJ, Mulder WJ, Fayad ZA, Cormode DP. 2013. Multifunctional gold nanoparticles for diagnosis and therapy of disease. *Mol Pharm* 10:831–47.
- Mrakic-Spota S, Gussoni M, Montorsi M, Porcelli S, Vezzoli A. 2012. Assessment of a standardized ROS production profile in humans by electron paramagnetic resonance. *Oxid Med Cell Longev* 2012:Article ID 973927.
- Nakano K, Saito K, Mine S, Matsushita S, Tanaka Y. 2007. Engagement of CD44 up-regulates Fas ligand expression on T cells leading to activation-induced cell death. *Apoptosis* 12:45–54.
- Niidome T, Yamagata M, Okamoto Y, Akiyama Y, Takahashi H, Kawano T, et al. 2006. PEG-modified gold nanorods with a stealth character for *in vivo* applications. *J Control Release* 114:343–7.
- Palmer SM, Burch LH, Trindade AJ, Davis RD, Herczyk WF, Reinsmoen NL, Schwartz DA. 2005. Innate immunity influences long-term outcomes after human lung transplant. *Am J Respir Crit Care Med* 171:780–5.
- Pellegrino T, Manna L, Kudera S, Liedl T, Koktysh D, Rogach AL, et al. 2004. Hydrophobic nanocrystals coated with an amphiphilic polymer shell: a general route to water soluble nanocrystals. *Nano Lett* 4:703.
- Ramirez AM, Nunley DR, Rojas M, Roman J. 2008. Activation of tissue remodeling precedes obliterative bronchiolitis in lung transplant recipients. *Biomark Insights* 3:351–9.
- Russell JH. 1995. Activation-induced death of mature T cells in the regulation of immune responses. *Curr Opin Immunol* 7:382–8.
- Sadauskas E, Jacobsen NR, Danscher G, Stoltenberg M, Vogel U, Larsen A, et al. 2009. Biodistribution of gold nanoparticles in mouse lung following intratracheal instillation. *Chem Cent J* 3:16.
- Shukla R, Bansal V, Chaudhary M, Basu A, Bhonde RR, Sastry M. 2005. Biocompatibility of gold nanoparticles and their endocytotic fate inside the cellular compartment: a microscopic overview. *Langmuir* 21:10644–54.
- Summers C, Rankin SM, Condliffe AM, Singh N, Peters AM, Chilvers ER. 2010. Neutrophil kinetics in health and disease. *Trends Immunol* 31:318–24.
- Sung JH, Ji JH, Park JD, Song MY, Song KS, Ryu HR, et al. 2011. Subchronic inhalation toxicity of gold nanoparticles. *Part Fibre Toxicol* 8:16.
- Todd JL, Palmer SM. 2011. Bronchiolitis obliterans syndrome: the final frontier for lung transplantation. *Chest* 140:502–8.
- Torres M, Hall FL, O'Neill K. 1993. Stimulation of human neutrophils with formyl-methionyl-leucyl-phenylalanine induces tyrosine phosphorylation and activation of two distinct mitogen-activated protein-kinases. *J Immunol* 150:1563–77.
- Uchiyama MK, Deda DK, Rodrigues SF, Drewes CC, Bolonheis SM, Kiyohara PK, et al. 2014. *In vivo* and *in vitro* toxicity and anti-inflammatory properties of gold nanoparticle bioconjugates to the vascular system. *Toxicol Sci* 142:497–507.
- Vanaudenaerde BM, Verleden SE, Vos R, De Vleeschauwer SI, Willems-Widyastuti A, Geenens R, et al. 2011. Innate and adaptive interleukin-17-producing lymphocytes in chronic inflammatory lung disorders. *Am J Respir Crit Care Med* 183:977–86.
- Verleden SE, Vasilescu DM, McDonough JE, Ruttens D, Vos R, Vandermeulen E, et al. 2015. Linking clinical phenotypes of chronic lung allograft dysfunction to changes in lung structure. *Eur Respir J* 46:1430–9.

- Weigt SS, DerHovanesian A, Wallace WD, Lynch JP 3rd, Belperio JA. 2013. Bronchiolitis obliterans syndrome: the Achilles' heel of lung transplantation. *Semin Respir Crit Care Med* 34:336–51.
- Wynn TA. 2011. Integrating mechanisms of pulmonary fibrosis. *J Exp Med* 208:1339–50.
- Yu LE, Yung LL, Ong C, Tan Y, Balasubramaniam KS, Hartono D, et al. 2009. Translocation and effects of gold nanoparticles after inhalation exposure in rats. *Nanotoxicology* 1:235.
- Zhao J, Wallace M, Melancon MP. 2014. Cancer theranostics with gold nanoshells. *Nanomedicine (Lond)* 9:2041–57.